§21. Dynamics of Zonal Flows in Helical Systems

Sugama, H., Watanabe, T.-H.

Zonal flows are observed in numerous natural systems such as atmospheric currents while in fusion science they are intensively investigated as an attractive mechanism for realizing a good plasma confinement. Rosenbluth and Hinton [1] showed that initial $\mathbf{E}\times\mathbf{B}$ rotation in tokamaks is not fully damped by collisionless processes but it approaches a finite value. Collisional decay of zonal flows occurs in the long course of time although the residual zonal flows in a collisionless time scale still influence the turbulent transport. Since zonal flows are a key issue for improved confinement in helical systems as well, it is necessary to examine how helical geometries affect zonal-flow damping. In the present work [2], collisionless zonal-flow dynamics in helical systems is investigated. In the same manner as in Rosenbluth and Hinton [1], we here treat the ITG turbulence as a known source and analytically derive the response kernel which relates the zonal-flow potential to the source and also represents dependence on an initially given zonal flow. We also verify the validity of the derived response kernel by a recently-developed gyrokinetic-Vlasov-simulation code.

In helical configurations, the radial drift motion of particles trapped in helical ripples yields neoclassical ripple transport in the weak collisionality regime. This radial drift also causes a significant difference between long-time zonal-flow behavior in helical systems and that in tokamaks. We define a characteristic transition time τ_c by $\tau_c \sim 1/|k_r \overline{v}_{dr}|$ where $\overline{v}_{dr}$ is the bounce-averaged radial drift velocity evaluated by considering helical-ripple-trapped thermal particles. When $t \ll \tau_c$, effects of the radial drift is weak and the long-time behavior of the zonal-flow potential is written as

$$\frac{e\phi_{\mathbf{k}_\perp}(t)}{T_i} = \mathcal{K}_< \left[\frac{e\phi_{\mathbf{k}_\perp}(0)}{T_i} + \frac{\int_0^t dt' \langle \int d^3v\, F_{i0} S_{i\mathbf{k}_\perp}(t') \rangle}{n_0 \langle k_\perp^2 a_i^2 \rangle} \right], \tag{1}$$

where $S_{\mathbf{k}_\perp}$ represents the $\mathbf{E}\times\mathbf{B}$ nonlinearity source term. Here, the response kernel $\mathcal{K}_<$ for $t \ll \tau_c$ is given by

$$\mathcal{K}_< = 1/(1+G) \tag{2}$$

where the geometrical factor G measures the ratio of the neoclassical polarization due to toroidally trapped particles to the classical polarization.

Next, when $t \gg \tau_c$, the density of nonadiabatic helical-ripple-trapped particles is strongly damped because of phase mixing caused by the bounce-averaged radial drift motion. Then, the long-time behavior of the zonal-flow potential for $t \gg \tau_c$ is given by

$$\begin{aligned} \frac{e\phi_{\mathbf{k}_\perp}(t)}{T_i} &= \mathcal{K}_> \left[\frac{e\phi_{\mathbf{k}_\perp}(0)}{T_i} \right. \\ &\left. + \frac{\int_0^t dt' \langle \int_{\kappa^2>1} d^3v\, F_{i0} S_{i\mathbf{k}_\perp}(t') \rangle}{n_0 \langle k_\perp^2 a_i^2 \rangle \{1-(2/\pi)\langle (2\epsilon_H)^{1/2}\rangle\}} \right], \end{aligned} \tag{3}$$

where the response kernel $\mathcal{K}_>$ for $t \gg \tau_c$ is given by

$$\begin{aligned} \mathcal{K}_> &= \langle k_\perp^2 a_i^2 \rangle \left[1-(2/\pi)\langle (2\epsilon_H)^{1/2}\rangle \right] \\ &\times \left\{ \langle k_\perp^2 a_i^2 \rangle [1-(3/\pi)\langle (2\epsilon_H)^{1/2}\rangle + G] \right. \\ &\left. + (2/\pi)(1+T_i/T_e)\langle (2\epsilon_H)^{1/2}\rangle \right\}^{-1}. \end{aligned} \tag{4}$$

Here, ϵ_H represents the helical-ripple parameter. A term with T_i/T_e appears in the response kernel $\mathcal{K}_>$ for $t \gg \tau_c$ because not only ions but also electrons influence the quasineutrality condition through their helical-ripple-bounce-averaged radial drift motion. The dependence on electrons and on the radial wave number shown in Eq. (4) is not seen in the tokamak case. In the axisymmetric limit $\epsilon_H \to +0$ with $\epsilon_T = \epsilon_t \cos\theta$, we obtain $G \to 1.6\, q^2/\epsilon_t^{1/2}$, which reduces both Eqs. (2) and (4) to the Rosenbluth-Hinton formula $\mathcal{K}_{\rm R-H} = 1/(1+1.6\, q^2/\epsilon_t^{1/2})$ [1].

Time evolution of the zonal-flow potential obtained by the simulation is plotted by a solid curve in Fig. 1, where $\epsilon_t = 0.1$, $\epsilon_h = 0.1$, $q = 1.5$, and $k_r a_i = 0.131$ are used. Here, a dashed horizontal line represents the response kernel $\mathcal{K}_>$ given by Eq. (4) for $t > \tau_c (= 7.6 R_0 v_{ti})$. It is seen that, after oscillations of the geodesic acoustic mode (GAM) are damped, the zonal-flow amplitude approaches the predicted value $\mathcal{K}_> = 0.038$, which is smaller than $\mathcal{K}_< = 0.39$ and $\mathcal{K}_{\rm R-H} = 0.081$ for the used parameters. Under the conditions used in our simulation, the GAM oscillations dominate the zonal-flow evolution for $t < \tau_c$ so that we cannot identify $\mathcal{K}_<$ given by Eq. (1) which describes the long-time behavior for $t \ll \tau_c$ with rapid phenomena such as the GAM neglected.

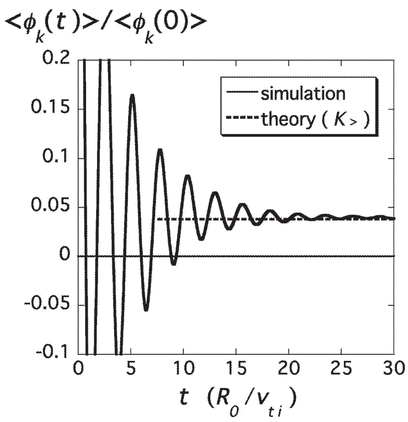

Fig.1. Time evolution of the zonal flow potential obtained by the gyrokinetic-Vlasov simulation for a helical system with $L = 2$, $M = 10$, $q = 1.5$, $\epsilon_t = \epsilon_h = 0.1$, and $k_r a_i = 0.131$. A dashed horizontal line corresponds to $\mathcal{K}_>$ given by Eq. (4) for $t > \tau_c$.

References

1) M. N. Rosenbluth and F. L. Hinton, Phys. Rev. Lett. **80**, 724 (1998).

2) H. Sugama and T.-H. Watanabe, Phys. Rev. Lett. **94**, 115001 (2005).